M.F. DIMIAN,[1] A.M. MEGAHED[2]

[1] Department of Mathematics, Ain Shams University, Faculty of Science
(Cairo, Egypt; e-mail: mouradfadl@yahoo.com, ah_mg_sh@yahoo.com)

[2] Department of Mathematics, Faculty of Science
(Benha University (13518), Egypt)

PACS 47.85.Dh, 62.20.+w, 65.20.Fe

EFFECTS OF VARIABLE FLUID PROPERTIES ON UNSTEADY HEAT TRANSFER OVER A STRETCHING SURFACE IN THE PRESENCE OF THERMAL RADIATION

The effect of radiation on the unsteady flow over a stretching surface with variable viscosity and variable thermal conductivity is analyzed. Similar governing equations are obtained by using suitable transformations and are then solved by applying the Chebyshev spectral method. Numerical results for the dimensionless velocity profiles and the dimensionless temperature are graphically presented for various values of the radiation parameter, viscosity, thermal conductivity, space and time indices, Prandtl number, and unsteadiness parameter. It is shown that both the skin friction and the rate of heat transfer decrease, as the Prandtl number and the unsteadiness parameter decrease. But both decrease, as the radiation parameter increases. The dimensionless temperature increases with the radiation parameter and the viscosity, but it decreases as the space and time indices increase.

Keywords: variable properties, thermal radiation, unsteady stretching sheet, Chebyshev spectral method.

1. Introduction

The continuous surface heat transfer problem has many practical applications in industrial manufacturing processes such as wire and fiber coating, food stuff processing, reactor fluidization, transpiration cooling, *etc.* Production of a thin liquid film either on the surface of a vertical wall by means of the action of gravity or on a rotating horizontal disk due to the action of centrifugal forces has been studied considerably in the literature (Sparrow and Gregg [1] and Dandapot and Ray [2, 3]). Ali [4] investigated the flow and heat transfer characteristics on a stretching surface using the power-law velocity and temperature distributions. A class of flow problems with the obvious relevance to the polymer extrusion is presented by the flows induced by the stretching motion of a flat elastic sheet. Crane [5] was the first who studied the motion set up in the ambient fluid due to a linearly stretching surface. Several authors (e.g., Gupta [6] and Tsou *et al.* [7]) subsequently explored various aspects of the accompanying heat transfer occurring in the infinite fluid medium surrounding the stretching sheet. They analyzed the stretching problem with a constant surface temperature, while Soundalgekar and Ramana [8] investigated the constant surface velocity case with a power-law temperature variation. Grubka and Bobba [9] analyzed the stretching problem for a surface moving with linear velocity and with variable surface temperature. Since the pioneer work by Sakiadis [10] who developed a numerical solution for the boundary layer flow field of a stretched surface, many authors have attacked this problem to study the hydrodynamic and thermal boundary layers due to a moving surface (e.g., Magyari and Keller [11]). The flow field of a stretching wall with a power-law velocity variation was discussed by Banks [12]. Ali [13] extended Bank's work to the case of a porous stretching surface for different values of the injection parameter. Abo-Eldahab and Gendy [14] investigated the solution for the steady flow in a boundary layer over the vertical stretching surface with internal heat generation. Heat transfer over an unsteady stretching surface with internal heat generation or absorption was studied by Elbashbeshy and Bazid [15]. They solved numerically the governing time-dependent boundary layer equations with constant viscosity. The momentum and heat transfer in a laminar liquid film on a horizontal stretching sheet was analyzed by Andersson *et al.* [16]. The governing time-dependent boundary layer equations are reduced to a set of ordinary differential equations by means of exact similarity transformations (which are used in [15]). The resulting problem (with constant viscosity) is solved numerically for some representative values of the unsteadiness parameter and the Prandtl number. Elbashbeshy and Dimian [17] studied the effect of radiation on the problem of flow and heat transfer over a wedge with variable viscosity. The effect of thermal radiation on the free convection flow and heat transfer over a variable plate in the presence of suction and injection was discussed by Hassain *et al.* [18]. Elshehawey *et al.* [19] investigated the problem of flow and heat transfer over an unsteady stretching sheet in a viscoelastic fluid with uniform suction at the wall and heat transfer in the presence of a normal magnetic field. Elbashbeshy and Aldawody [20] investigated the effects of thermal radiation and a magnetic field on the unsteady boundary layer mixed convection flow and the heat transfer from a vertical porous stretching surface. Bataller [21] presented the effects of a non-uniform heat source on the viscoelastic fluid flow and heat transfer over a stretching sheet. The purpose of the present paper is to explore the effect of radiation on the unsteady flow over a stretching surface with variable properties. Accurate numerical solutions will be provided for various values of radiation parameter, viscosity, the unsteadiness parameter, and the Prandtl number.

2. Formulation of the Problem

Consider the unsteady two-dimensional laminar boundary layer flow over a stretching sheet immersed in an incompressible fluid. The x axis is chosen along the plane of the sheet, and the y axis is taken to be normal to the plane. We assume that the surface starts stretching from rest with a velocity $U(x,t)$. The viscosity and the thermal conductivity of the fluid is assumed to vary with the temperature as follows (Mahmoud and Megahed [22]):

$$\mu = \mu_\infty e^{-\alpha\theta}, \tag{1}$$

$$\kappa = \kappa_\infty(1+\epsilon\theta), \tag{2}$$

where μ_∞, κ_∞ are the cofficients of viscosity and thermal conductivity at the ambient, α is the viscosity parameter and ϵ is the thermal conductivity parameter. The governing time-dependent boundary layer equations for mass, momentum, and energy conservation are given by

$$\frac{\partial u}{\partial x} + \frac{\partial v}{\partial y} = 0, \tag{3}$$

$$\frac{\partial u}{\partial t} + u\frac{\partial u}{\partial x} + v\frac{\partial u}{\partial y} = \frac{1}{\rho}\frac{\partial}{\partial y}\left(\mu\frac{\partial u}{\partial y}\right), \tag{4}$$

$$\frac{\partial T}{\partial t} + u\frac{\partial T}{\partial x} + v\frac{\partial T}{\partial y} = \frac{1}{\rho c_p}\frac{\partial}{\partial y}\left(\kappa\frac{\partial T}{\partial y}\right) - \frac{1}{\rho c_p}\left(\frac{\partial q_r}{\partial y}\right), \tag{5}$$

where u and v are the velocity components along the x and y directions, respectively, t is the time, ρ is the fluid density, μ is the viscosity, κ is the thermal conductivity, T is the temperature of the fluid, q_r is the radiative heat flux, and c_p is the specific heat at constant pressure. The appropriate boundary conditions for the present problem are

$$u = U, \quad v = 0, \quad T = T_w \quad \text{at} \quad y = 0, \tag{6}$$

$$u \to 0, \quad T \to T_\infty \quad \text{as} \quad y \to \infty, \tag{7}$$

where U is the surface velocity of the stretching sheet, T_w is the surface temperature, T_∞ is the free stream temperature, and the flow is caused by stretching the elastic surface at $y = 0$ such that the continuous sheet moves in the x direction with the velocity

$$U = \frac{bx}{1-at}, \tag{8}$$

where a and b are positive constants with dimension (time^{-1}). Our problem is valid only for $at \ll 1$, but $at \succeq 1$ has no physical meaning.

The radiative heat flux q_r is employed according to the Roseland approximation [23] such that

$$q_r = -\frac{4\sigma^*}{3k^*}\frac{\partial T^4}{\partial y}, \tag{9}$$

where σ^* is the Stefan–Boltzmann constant, and k^* is the mean absorption coefficient. Following Raptis [24], we assume that the temperature differences within the flow are small and such that may be expressed as a linear function of the temperature. Expanding T^4 in a Taylor series about T_∞ and neglecting higher-order terms, we have

$$T^4 \cong 4T_\infty^3 T - 3T_\infty^4. \tag{10}$$

The equation of continuity is satisfied if we choose a stream function $\psi(x, y)$ such that $u = \frac{\partial\psi}{\partial y}$, and $v = -\frac{\partial\psi}{\partial x}$. The mathematical analysis of the problem is simplified by introducing the following dimensionless coordinates:

$$\eta = \left(\frac{b}{(\mu_\infty/\rho)}\right)^{1/2}(1-at)^{-1/2}y, \tag{11}$$

$$\psi = \left(\frac{\mu_\infty b}{\rho}\right)^{1/2}(1-at)^{-1/2}xf(\eta), \tag{12}$$

$$T = T_\infty + T_0\left(\frac{dx^r}{2(\mu_\infty/\rho)}\right)(1-at)^{-m}\theta(\eta), \tag{13}$$

$$T_w = T_\infty + T_0\left(\frac{dx^r}{2(\mu_\infty/\rho)}\right)(1-at)^{-m}. \tag{14}$$

Here, f is the dimensionless stream function, θ is the dimensionless temperature of the fluid, d is constant, and r and m are space and time indices, respectively.

Using Eqs. (11)–(14), the mathematical problem defined in Eqs. (4), (5) is then transformed into a set of ordinary differential equations with the associated boundary conditions:

$$e^{-\alpha\theta}(f''' - \alpha\theta' f'') + ff'' - \frac{S}{2}\eta\, f'' - f'^2 - Sf' = 0, \tag{15}$$

$$\frac{1}{\Pr}[(1+R+\epsilon\theta)\theta'' + \epsilon\theta'^2] + $$

$$+ f\theta' - rf'\theta - S\left(\frac{1}{2}\eta\theta' + m\theta\right) = 0, \tag{16}$$

$$f(0) = 0, \quad f'(0) = 1, \quad \theta(0) = 1, \tag{17}$$

$$f' \to 0, \quad \theta \to 0 \quad as \quad \eta \to \infty, \tag{18}$$

where the prime denotes the differentiation with respect to η, $\theta = \frac{T-T_\infty}{T_w-T_\infty}$ is the dimensionless temperature, $S = a/b$ is the unsteadiness parameter, $\Pr = \frac{\rho\nu c_p}{\kappa_\infty}$ is the Prandtl number, and $R = \frac{16\sigma^* T_\infty^3}{3k^*\kappa_\infty}$ is the radiation parameter.

The physical quantities of interest are the skin-friction coefficient C_f and the local Nusselt number Nu_x which are defined as

$$C_f = -2\mathrm{Re}_x^{-1/2} f''(0),$$

$$\mathrm{Nu}_x = -\frac{1}{2}(1-at)^{-1/2}\mathrm{Re}_x^{3/2}\theta'(0), \tag{19}$$

where $\mathrm{Re}_x = \frac{\rho U x}{\mu}$ is the local Reynolds number.

3. Method of Solution

The domain of the governing boundary layer equations (15), (16) is the unbounded region $[0, \infty)$. However, for all practical reasons, this could be replaced by the interval $0 \le \eta \le \eta_\infty$, where η_∞ is some large number to be specified for the computational convenience. Using the algebraic mapping

$$\chi = 2\frac{\eta}{\eta_\infty} - 1,$$

the unbounded region $[0, \infty)$ is finally mapped onto the finite domain $[-1, 1]$, and the problem expressed by Eqs. (15) and (16) is transformed into

$$e^{-\alpha\theta(\chi)}[f'''(\chi) - \alpha\theta(\chi)f''(\chi)] +$$

$$+\left(\frac{\eta_\infty}{2}\right) f(\chi)f''(\chi) - \left(\frac{\eta_\infty}{2}\right) f'^2(\chi) -$$

$$-S\left[\left(\frac{\eta_\infty}{8}\right)(\chi+1)f''(\chi) + \left(\frac{\eta_\infty}{2}\right)^2 f'(\chi)\right] = 0, \tag{20}$$

$$\frac{1}{\Pr}[(1+R+\epsilon\theta(\chi))\theta''(\chi) + \epsilon\theta'(\chi)^2] +$$

$$+\left(\frac{\eta_\infty}{2}\right) f(\chi)\theta'(\chi) - r\left(\frac{\eta_\infty}{2}\right) f'(\chi)\theta(\chi) -$$

$$-S\left[\left(\frac{\eta_\infty}{8}\right)(\chi+1)\theta'(\chi) + m\left(\frac{\eta_\infty}{2}\right)^2 \theta(\chi)\right] = 0. \tag{21}$$

The transformed boundary conditions are

$$f(-1) = 0, \quad f'(-1) = \left(\frac{\eta_\infty}{2}\right), \quad \theta(-1) = 1, \tag{22}$$

$$f'(1) = 0, \quad \theta(1) = 0, \tag{23}$$

where the differentiation in Eqs. (20) and (21) will be with respect to the new variable χ. Our technique is accomplished by starting with the Chebyshev approximation for the highest order derivatives, f''' and θ'', and generating approximations to the lower order derivatives f'', f', f, θ', and θ as follows: Setting $f''' = \phi(\chi)$, and $\theta'' = \zeta(\chi)$ and then integrating we obtain

$$f''(\chi) = \int_{-1}^{\chi} \phi(\chi) d\chi + C_1^f, \tag{24}$$

$$f'(\chi) = \int_{-1}^{\chi}\int_{-1}^{\chi} \phi(\chi) d\chi d\chi + C_1^f(\chi+1) + C_2^f, \tag{25}$$

$$f(\chi) = \int_{-1}^{\chi}\int_{-1}^{\chi}\int_{-1}^{\chi} \phi(\chi) d\chi d\chi d\chi +$$

$$+ C_1^f \frac{(\chi+1)^2}{2} + C_2^f(\chi+1) + C_3^f, \tag{26}$$

$$\theta'(\chi) = \int_{-1}^{\chi} \zeta(\chi) d\chi + C_1^\theta, \tag{27}$$

$$\theta(\chi) = \int_{-1}^{\chi}\int_{-1}^{\chi} \zeta(\chi) d\chi d\chi + C_1^\theta(\chi+1) + C_2^\theta. \tag{28}$$

From the boundary conditions (22) and (23), we have

$$C_1^f = -\frac{1}{2}\int_{-1}^{1}\int_{-1}^{\chi} \phi(\chi) d\chi d\chi, \quad C_2^f = \left(\frac{\eta_\infty}{2}\right), \quad C_3^f = 0,$$

$$C_1^\theta = -\frac{1}{2} - \frac{1}{2}\int_{-1}^{1}\int_{-1}^{\chi} \zeta(\chi) d\chi d\chi, \quad C_2^\theta = 1.$$

Therefore, we can give approximations to Eqs. (20) and (21) as follows:

$$f_i(\chi) = \sum_{j=0}^{n} l_{ij}^f \phi_j + d_i^f, \quad f_i'(\chi) = \sum_{j=0}^{n} l_{ij}^{f1} \phi_j + d_i^{f1},$$

$$f_i''(\chi) = \sum_{j=0}^{n} l_{ij}^{f2} \phi_j + d_i^{f2}, \tag{29}$$

$$\theta_i(\chi) = \sum_{j=0}^{n} l_{ij}^\theta \zeta_j + d_i^\theta, \quad \theta_i'(\chi) = \sum_{j=0}^{n} l_{ij}^{\theta 1} \zeta_j + d_i^{\theta 1}, \tag{30}$$

for all $i = 0(1)n$, where

$$l_{ij}^f = b_{ij}^3 - \frac{1}{2}\frac{(\chi_i+1)^2}{2} b_{nj}^2, \quad d_i^f = (\chi_i+1)\left(\frac{\eta_\infty}{2}\right),$$

$$l_{ij}^{f1} = b_{ij}^2 - \frac{1}{2}(\chi_i+1) b_{nj}^2, \quad d_i^{f1} = \frac{\eta_\infty}{2},$$

$$l_{ij}^{f2} = b_{ij} - \frac{1}{2} b_{nj}^2, \quad d_i^{f2} = 0,$$

$$l_{ij}^{\theta} = b_{ij}^2 - \frac{1}{2}(\chi_i+1) b_{nj}^2, \quad d_i^{\theta} = 1 - \frac{1}{2}(\chi_i+1),$$

$$l_{ij}^{\theta 1} = b_{ij} - \frac{1}{2} b_{nj}^2, \quad d_i^{\theta 1} = -\frac{1}{2},$$

and $b_{ij}^2 = (\chi_i - \chi_j) b_{ij}$ and b_{ij} are the elements of the matrix B as given in [25]. By using Eqs. (29) and (30), one can transform Eqs. (20) and (21) to the following system of nonlinear equations with the highest derivatives:

$$e^{-\alpha(\sum_{j=0}^{n} l_{ij}^\theta \zeta_j + d_i^\theta)}\Big(\phi_i - \alpha\Big(\sum_{j=0}^{n} l_{ij}^{\theta 1}\zeta_j + d_i^{\theta 1}\Big)\times$$

$$\times\Big(\sum_{j=0}^{n} l_{ij}^{f2}\phi_j + d_i^{f2}\Big)\Big) + \Big(\frac{\eta_\infty}{2}\Big)\Big(\sum_{j=0}^{n} l_{ij}^{f}\phi_j + d_i^{f}\Big)\times$$

$$\times\Big(\sum_{j=0}^{n} l_{ij}^{f2}\phi_j + d_i^{f2}\Big) - \Big(\frac{\eta_\infty}{2}\Big)(\sum_{j=0}^{n} l_{ij}^{f1}\phi_j + d_i^{f1}\Big)^2 -$$

$$-S\Big[\Big(\frac{\eta_\infty}{8}\Big)(\chi_i+1)\Big(\sum_{j=0}^{n} l_{ij}^{f2}\phi_j + d_i^{f2}\Big) +$$

$$+\Big(\frac{\eta_\infty}{2}\Big)^2\Big(\sum_{j=0}^{n} l_{ij}^{f1}\phi_j + d_i^{f1}\Big)\Big] = 0, \tag{31}$$

$$\frac{1}{\Pr}\Big[\Big(1+R+\epsilon\Big(\sum_{j=0}^{n} l_{ij}^{\theta}\zeta_j + d_i^{\theta}\Big)\Big)\zeta_i + \epsilon\Big(\sum_{j=0}^{n} l_{ij}^{\theta 1}\zeta_j + d_i^{\theta 1}\Big)^2\Big] +$$

$$+\Big(\frac{\eta_\infty}{2}\Big)\Big(\sum_{j=0}^{n}(l_{ij}^{f}\phi_j + d_i^{f}\Big)\Big(\sum_{j=0}^{n} l_{ij}^{\theta 1}\zeta_j + d_i^{\theta 1}\Big) -$$

$$-r\Big(\frac{\eta_\infty}{2}\Big)\Big(\sum_{j=0}^{n} l_{ij}^{f1}\phi_j + d_i^{f1}\Big)\Big(\sum_{j=0}^{n} l_{ij}^{\theta}\zeta_j + d_i^{\theta}\Big) -$$

$$-S\Big[\Big(\frac{\eta_\infty}{8}\Big)(\chi_i+1)\Big(\sum_{j=0}^{n} l_{ij}^{\theta 1}\zeta_j + d_i^{\theta 1}\Big) +$$

$$+m\Big(\frac{\eta_\infty}{2}\Big)^2\Big(\sum_{j=0}^{n} l_{ij}^{\theta}\zeta_j + d_i^{\theta}\Big)\Big] = 0. \tag{32}$$

This system is then solved with the use of Newton's iteration.

4. Results and Discussion

The effect of the unsteadiness parameter S on the velocity distribution is shown in Fig. 1. It is worth to note that the velocity profile decreases with increase in the value of unsteadiness parameter. The effect of the unsteadiness parameter S on the temperature can be seen from Fig. 2. The temperature decreases, as S increases. This shows the important fact that the rate of cooling is much faster for the higher values of unsteadiness parameter; whereas it may take longer time of cooling for smaller values of unsteadiness parameter. Figure 3 illustrates the effect of the viscosity parameter α on the velocity profile. It can be shown that the velocity decreases along the surface with increase in the viscosity parameter. But the temperature $\theta(\eta)$ increases with the viscosity parameter, as shown in Fig. 4. The effect of the thermal

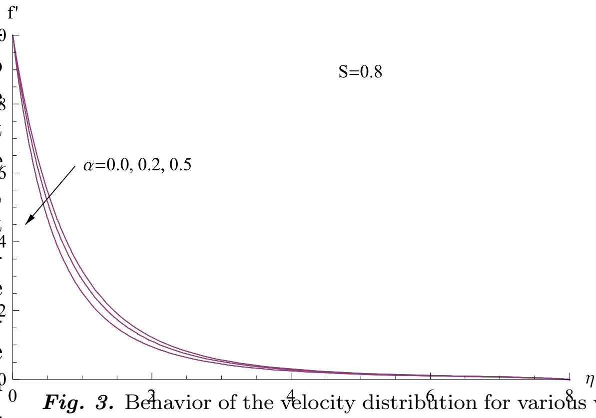

Fig. 3. Behavior of the velocity distribution for various values of α

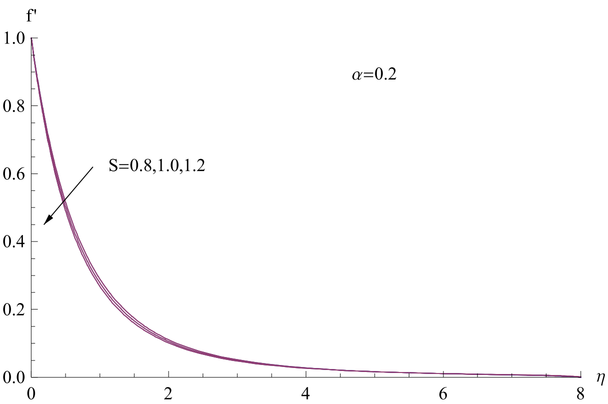

Fig. 1. Behavior of the velocity distribution for various values of S

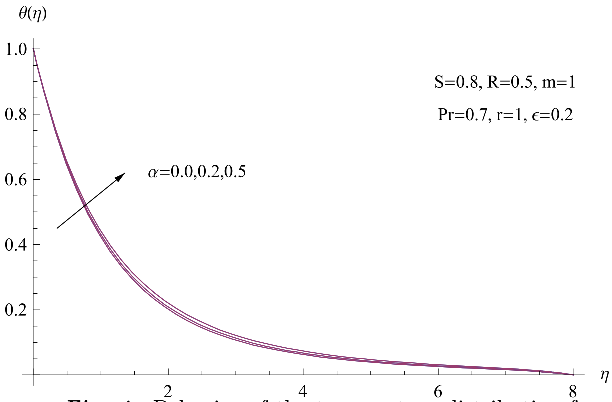

Fig. 4. Behavior of the temperature distribution for various values of α

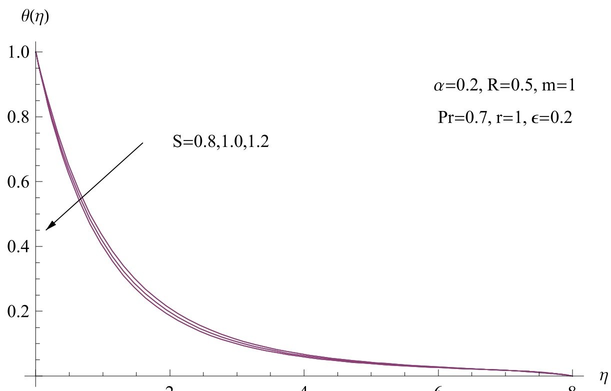

Fig. 2. Behavior of the temperature distribution for various values of S

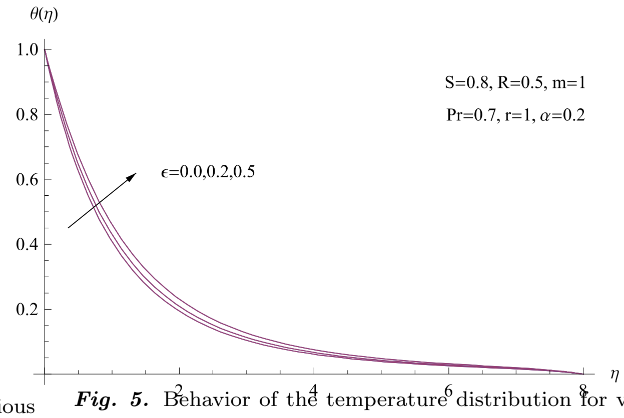

Fig. 5. Behavior of the temperature distribution for various values of ϵ

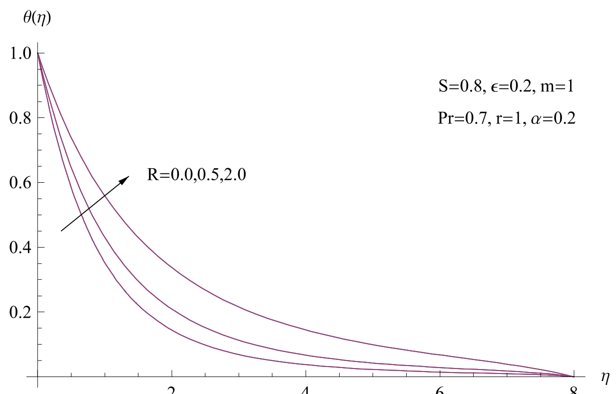

Fig. 6. Behavior of the temperature distribution for various values of R

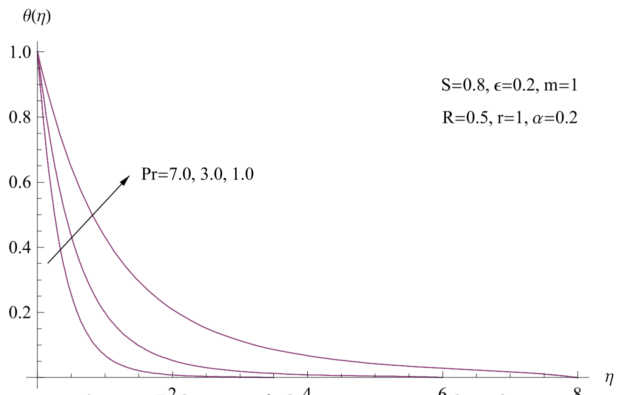

Fig. 7. Behavior of the temperature distribution for various values of Pr

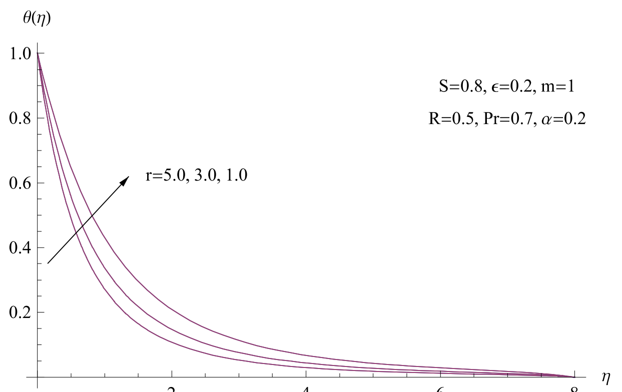

Fig. 8. Behavior of the temperature distribution for various values of r

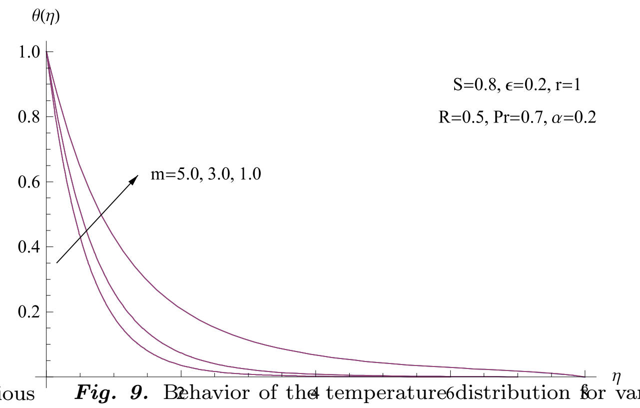

Fig. 9. Behavior of the temperature distribution for various values of m

Variation of $-f''(0)$ and $-\theta'(0)$ for various values of S, α, ϵ, R, Pr, r, and m

S	α	ϵ	R	Pr	r	m	$-f''(0)$	$-\theta'(0)$
0.8	0.2	0.2	0.5	0.7	1.0	1.0	1.42402	0.907794
1.0	0.2	0.2	0.5	0.7	1.0	1.0	1.49170	0.956017
1.2	0.2	0.2	0.5	0.7	1.0	1.0	1.55672	1.00182
0.8	0.0	0.2	0.5	0.7	1.0	1.0	1.26104	0.919437
0.8	0.2	0.2	0.5	0.7	1.0	1.0	1.42402	0.907794
0.8	0.5	0.2	0.5	0.7	1.0	1.0	1.69893	0.889748
0.8	0.2	0.0	0.5	0.7	1.0	1.0	1.42582	0.990991
0.8	0.2	0.2	0.5	0.7	1.0	1.0	1.42402	0.907794
0.8	0.2	0.5	0.5	0.7	1.0	1.0	1.42175	0.811629
0.8	0.2	0.2	0.0	0.7	1.0	1.0	1.42915	1.09841
0.8	0.2	0.2	0.5	0.7	1.0	1.0	1.42402	0.907794
0.8	0.2	0.2	2.0	0.7	1.0	1.0	1.4162	0.636417
0.8	0.2	0.2	0.5	1.0	1.0	1.0	1.4325	0.97994
0.8	0.2	0.2	0.5	3.0	1.0	1.0	1.44197	1.68237
0.8	0.2	0.2	0.5	7.0	1.0	1.0	1.46038	2.66888
0.8	0.2	0.2	0.5	0.7	1.0	1.0	1.42402	0.907794
0.8	0.2	0.2	0.5	0.7	3.0	1.0	1.43163	1.26733
0.8	0.2	0.2	0.5	0.7	5.0	1.0	1.43755	1.57237
0.8	0.2	0.2	0.5	0.7	1.0	1.0	1.42402	0.907794
0.8	0.2	0.2	0.5	0.7	1.0	3.0	1.43555	1.34684
0.8	0.2	0.2	0.5	0.7	1.0	5.0	1.4423	1.66032

conductivity parameter ϵ on the temperature profile θ is presented in Fig. 5. From this figure, it can be seen that the temperature distribution increases with the thermal conductivity parameter. Figure 6 represents the effect of the radiation parameter R on the dimensionless temperature. It is clear that the temperature increases with the radiation parameter. So, it can be seen that the thermal boundary layer increases with the radiation parameter R. This result agrees with Elbashbeshy and Dimian [17] in their special case (wedge angle is zero). The effect of the Prandtl number on the temperature distribution is demonstrated in Fig. 7. It can be observed that the temperature profiles decrease for the increasing values of Prandtl number. This is in agreement with the physical fact that the thermal boundary layer thickness decreases with increase of Pr. The influence of the space index r on temperature variations is shown in Fig. 8, which demonstrates that the temperature raises to a higher value, as S decreases. This corresponds to the more strong intensity of a heat flux specified at the surface. Likewise, the temperature turns to a lower value, as m increases, which is observed from Fig. 9. Table presents the values of skin-friction coefficient and local Nusselt number for various values of the parameters governing the flow and the heat transfer. Based on this table, we note that the skin friction coefficient and the local Nusselt number increase with the unsteadiness parameter, space index, time index, and Prandtl number. Likewise, the local Nusselt number decreases with increase of the viscosity parameter, thermal conductivity parameter, and radiation parameter. Finally, the skin-friction coefficient is found to be increased with the viscosity parameter, but the reverse is true for the variable thermal conductivity parameter.

5. Conclusions

Numerical solutions have been obtained to study the effect of variable fluid properties on the flow and the heat transfer in the laminar flow of an incompressible fluid past an unsteady stretching surface in the presence of thermal radiation. The obtained similarity ordinary differential equations are solved numerically by using the Chebyshev spectral method. It is found that

1. The skin friction coefficient increases with the unsteadiness parameter, viscosity parameter, space and time indices, and Prandtl number, but it decreases, as the thermal conductivity parameter and the radiation parameter decrease.

2. The Nusselt number coefficient increases with the unsteadiness parameter, Prandtl number, and space and time indices, but it decreases, as the viscosity parameter, thermal conductivity parameter and radiation parameter decrease.

3. The dimensionless velocity and the dimensionless temperature decrease, as unsteadiness parameter increases.

4. The dimensionless velocity and the dimensionless temperature increase, as the radiation parameter increases, but the effect on the velocity is very weak.

1. E.M. Sparrow and J.I. Gregg, ASME J. Heat Transfer **81**, 13 (1959).
2. B.S. Dandapat and P.C. Ray, Int. J. Non-Linear Mech. **25**, 569 (1990).
3. B.S. Dandapat and P.C. Ray, J. Phys. D. Appl. Phys. **27**, 2041 (1994).
4. M. E. Ali, Warme- und Stoff. **29**, 227 (1994).
5. L.J. Crane, Z. Angew Math. Phys. **21**, 645 (1970).
6. P.S. Gupta and A.S. Gupta, Can. J. Chem. Eng. **55**, 744 (1977).
7. F.K. Tsou, E.M. Sparrow, and R.J. Goldstein, Int. J. Heat Mass Transfer **10**, 219 (1967).
8. V.M. Soundalgekar and T.V. Ramana Murty, Warme- und Stoff. **14**, 91 (1980).
9. L.J. Grubka and K.M. Bobba, AME J. Heat Transfer **107**, 248 (1985).
10. B.C. Sakiadis, A.I.Ch.E. Journ. **7**, 26 (1961).
11. E. Magyari and B. Keller, J. Phys. D. Appl. Phys. **32**, 2876 (1999).
12. W.H.H. Banks, J. Mec. Theor. Appl. **2**, 375 (1983).
13. M.E. Ali, Int. J. Heat Fluid Flow **16**, 280 (1995).
14. E.M. Abo-Eldahab and M.S. Elgendy, Phys. Scripta **62**, 321 (2000).
15. E.M.A. Elbashbeshy and M.A.A. Bazid, Appl. Math. Comp. **138**, 239 (2003).
16. H.I. Andersson, J.B. Aarseth, and B.S. Dandapat, Int. J. Heat Mass Transfer **43**, 69 (2000).
17. E.M.A. Elbashbeshy and M.F. Dimian, J. Appl. Math. and Comput. **132**, 445 (2002).
18. M.A. Hassain, M.A. Alin, and D.A.S. Rees, Int. J. Heat Mass Transfer **42**, 181 (1999).
19. E.F. Elshehawey, M.A. Kamel, and F.N. Ibrahim, Engin. Trans. (Polish Acad. Sci.) **33**, 299 (1985).
20. E.M.A. Elbashbeshy and D.A. Aldawody, Int. J. of Nonlinear Science **9**, 448 (2010).
21. R.C. Bataller, Int. J. Heat Mass Transfer **50**, 3152 (2007).
22. M.A.A. Mahmoud and A.M. Megahed, Can. J. Phys. **87**, 1065 (2009).
23. A. Raptis, Int. J. Heat Mass Transfer **41**, 2865 (1998).
24. A. Raptis, Int. Comm. Heat Mass Transfer **26**, 889 (1999).
25. S.E. El-Gendi, Computer J. **12**, 282 (1969).

Received 13.05.12

М.Ф. Діміан, А.М. Мегахед

ВПЛИВ ЗМІННИХ ВЛАСТИВОСТЕЙ РІДИНИ НА НЕСТАЦІОНАРНУ ТЕПЛОПЕРЕДАЧУ НАД РОЗТЯЖНОЮ ПОВЕРХНЕЮ В ПРИСУТНОСТІ ТЕПЛОВОГО ВИПРОМІНЮВАННЯ

Р е з ю м е

Досліджено вплив випромінювання на нестаціонарний потік над розтяжною поверхнею з мінливою в'язкістю і змінною теплопровідністю. Відповідні визначальні рівняння отримано з використанням відповідних перетворень і потім вирішені спектральним методом Чебишева. На графіках наведено результати розрахунків профілів безрозмірної швидкості та безрозмірної температури для різних значень параметра випромінювання, в'язкості, теплопровідності, індексів простору-часу, числа Прандтля і параметра нестаціонарності. Показано, що скін-тертя і швидкість теплопередачі зменшуються із зменшенням числа Прандтля і параметра нестаціонарності при зростанні параметра випромінювання. Безрозмірна температура зростає із збільшенням параметра випромінювання і в'язкості, але зменшується при збільшенні індексів простору-часу.